Published by Nigerian Society of Physical Sciences. Hosted by FLAYOO Publishing House LTD

Recent Advances in Natural Sciences

Journal Homepage: https://flayoophl.com/journals/index.php/rans

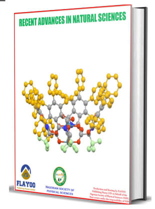

Examination of the potential for geothermal energy in parts of the Benue trough, Nigeria, through the use of high-resolution aeromagnetic data

Joseph Aza Ahile[a,*], Osita Chukwudi Meludu[a], Adetola Sunday Oniku[a], Sebastian Abraham Sunu[a], Lucky Peter Kenda[b], Simon Kwarki[c], Joseph Orojah Osumeje[d]

[a] *Department of Physics, Modibbo Adama University, Yola, Adamawa State, Nigeria*
[b] *Department of Physics, Taraba State University, Jalingo, Taraba state, Nigeria*
[c] *Department of Physics Education, Federal College of Education (Technical), Gombe, Gombe State, Nigeria.*
[d] *Department of Physics, Ahmadu Bello University, Zaria, Kaduna state, Nigeria*

ARTICLE INFO

Article history:
Received: 29 August 2024
Received in revised form: 30 October 2024
Accepted: 09 November 2024
Available online: 28 November 2024

Keywords: High-Resolution data, Curie Point Depth, Geothermal gradient, thermal transfer, Geothermal potentials

DOI:10.61298/rans.2024.2.2.124

ABSTRACT

Aeromagnetic data from nine sheets covering parts of Benue Trough Nigeria were analyzed to identify potential geothermal locations. The aeromagnetic data sheets were analyzed with Oasis Montaj 8.4, Matlab 7.5, Arcmap 10.7.1, and Surfer 13 combined. The centroid depth method was used to spectrally evaluate the depth of high-resolution aeromagnetic data. The findings showed that the research area's geothermal heat flow values range from 88.52259 mW/m^2 to 166.2844 mW/m^2, while the Curie Point Depth values range from 8.55 km to 16.38 km with a mean depth of 12.2068 km. The Geothermal Gradient values vary from 35.40904 ℃/km to 66.51376 ℃/km with a mean value of 48.85639 ℃/km. The region's mean thermal transfer is 122.1410 mW/m^2. It appears that the Curie Point Depth is highest for the lowest thermal transfer values and lowest for the highest thermal transfer values. The study area's heat flow measurements indicate that the crust is oceanic. The comprehensive geothermal data provided by this study may aid in the study area's geothermal energy exploitation. Given the extremely high heat flow recorded, there is a likelihood that the studied area has geothermal energy sources. As a result, it was observed that practically the entire study region had substantial heat flow (>80 mW/m^2), suggesting the possibility of a geothermal energy source.

1. INTRODUCTION

Due to the urgent need to move toward an environmentally friendly future and the threat posed by global warming, most developed nations, including those in the West and, more recently, some Asian nations, are in a race to find renewable energy sources and alternatives. Developing nations, on the other hand, have not even reached the point of meeting their most basic energy needs [1]. Concerns about resource depletion and the early signs of climate change have been raised by scientists and society, and these issues require immediate response. The majority of the country likely possesses untapped geothermal energy resources that might provide a stable and sustainable alternative energy source [2]. The Southwestern and Northcentral regions of the country, where hot and warm spots are found, appear to have

*Corresponding author: Tel.: +234-810-1500-437.
e-mail: ahilejoseph@gmail.com (Joseph Aza Ahile)

a wealth of renewable energy resources [2–4]. When these resources are properly and effectively utilized, they will provide a sustainable, dependable, and alternative energy source that will help address the problem of an intermittent energy supply and lessen the excessive reliance on petroleum and petroleum products, which has a detrimental effect on the ecosystem.

Geothermal energy is an energy source that is stored as heat beneath the solid portion of the ground [5]. The Earth's crust's geothermal energy is stable since it is independent of weather and comes from two sources: the planet's primordial emergence (20%) and radioactive substances disintegration (80%). The planet's base and top have different temperatures, which causes thermal energy to continuously condense as heat from the core to the surface. This phenomenon is known as the geothermal gradient. Whenever there is enough porosity to allow geothermal fluids to emerge to the outermost layer of the earth and spew, geothermal sources will always have surface manifestations [6].

Magnetic data has been effectively used by geoscientists to investigate geothermal energy resources in Nigeria. Ikumbur *et al*. [7] did analysis of the Middle Benue region of Nigeria's geothermal energy prospects using an aeromagnetic and Aeroradiometric technique. Their quantitative interpretation reveals that the depth to anomalous magnetic sources ranges between 0.76 and 4.46 km; while the depth to centroid ranges between 7.29-19.679 km. There is variation in the CPD between 12.70 and 37.22 km, the geothermal gradient between 15.58 and 45.670 C/km, and the geothermal heat flow between 38.9 and 114.17 mW/m^2. Ifeanyi *et al.* [8] assessed the Solid Mineral Potential and Geothermal Energy Reserve of the Northern Basement Complex, Nigeria. The spectral analysis of the Northern basement complex, Nigeria revealed the existence of two major source depths. The shallow sources in the second segment of the spectral layer have an average depth of 0.140 km and range in depth from 0.135 km to 0.201 km. The average depth to the basement or deeper source is 1.882 km, with a range of 1.655 km to 2.021 km. In thermally normal continental regions, the average heat flow has been estimated to be greater than 60 mW/m^2. Akiishi *et al.* [9] also investigated Curie point depth, geothermal gradient as well as heat flow in Masu, which is located within the Nigerian sector of Chad Basin spectral analysis. Their findings demonstrated that the area's Curie point depth obtained ranges from 12.233 km to 16.184 km with an average of 13.993 km, geothermal gradient ranges from 35.838 °C/km to 47.413 °C/km, with an average of 41.821°C/km, and the heat flow ranges from 8980 mWm $^{-2}$ to 117.80 mWm^{-2}, with an average of 104.551 mWm^{-2}.

Akinnubi & Adetona [10] investigated geothermal potential within Benue state, central Nigeria, from radiometric and high-resolution aeromagnetic data. Their spectral analysis indicates that there are variations in the depths to the top and bottom of magnetic sources, ranging from 0.28 km to 0.36 km and 5.52 km to 9.63 km, respectively. The average geothermal heat flow in the analyzed region is 103.98 mWm^{-2}, with a shallow Curie depth of 9 km in the southwestern and southeastern parts of the study area. Odidi *et al.* [11] did an investigative study on the geothermal energy potential of parts of central and northeastern Nigeria using a spectral analysis technique. Their findings indicate that the curie point depths (Zb) range from 7.6341 km to 34.5158 km, with a mean value of 14.7928 km; the geothermal gradient ranges from 16.8039 °Ckm^{-1} to 75.97490C km^{-1}, with a mean value of 45.7021 °Ckm^{-1}; and the heat flow (q) ranges from 42.0097 mWm^{-2} to 189.9372 mWm^{-2}, with a mean value of 114.2554 mWm^{-2} while Mohammed *et al.* [12] did assessment of Geothermal potentials in some parts of Upper Benue Trough Northeast Nigeria using Aeromagnetic data. According to the results of the 77 spectral analyses, the centroid depth in the Upper Benue trough varies from 7.26 to 18.00 km, while the basement depth varies from 0.55 to 3.8 km in the southwestern region towards the Lau area. The corresponding geothermal gradient and heat flow values range from 17.10 to 46.66 °C/km with an average of 30.75 °C/km and 42.75 to 116.65 mW/m^2 with an average of 75.91 mW/m^2, respectively, from the same section of the trough. The Curie point depths vary from 12.43 to 33.91 km.

Ibe & Uche [13] assessed the Geothermal Energy Potential of Ruwan Zafi, Adamawa State, and Environs, Northeastern Nigeria, using High-Resolution Airborne Magnetic Data. Within the study area, the upper boundary to magnetic bodies was estimated at depths ranging from 89.62 to 235.38 m, and the range of sediment thickness was determined by spectral analysis of the magnetic dataset. The estimated basal depth ranged from 8.40 to 17.16 km, the geothermal gradient from 33.79 to 69.01 °C/km, and the related mantle heat flow from approximately 84.48 mW/m^2 to 172.53 mW/m^2. Anyadiegwu & Aigbogun [14] also evaluated the aeromagnetic data over parts of the Lower Benue Trough and Anambra Basin of North Central and Southeastern Nigeria. According to their findings, the study area's average Curie point depth is 8.07594 km, and the average geothermal gradient is 73 °C/km. The locations with low and moderate geothermal gradients are Awgu, Northeast of Obi, Southeast of Obubra, and North West of Odolu. The average heat flow in the research area is 170 mW/m^2.

Recently, Egwuonwu *et al.* [15] estimated the Geothermal Energy Potentials within the Central Benue Trough Nigeria using Airborne Potential Field Data. Their findings indicated that the Curie point depth varied between 8.61 and 36.04 km, with an average depth of 14.81 km. Additionally, the geothermal gradient varied between 16.09 and 70.81 °C/km, with an average value of 45.39 °C/km. Lastly, the heat flow varied between 40.23 and 177.03 mWm^{-2}, with an average value of 113.49 mWm^{-2}. Salako *et al.* [16] also assessed geothermal potential in parts of the middle Benue Trough, northeast of Nigeria. The study's findings demonstrated that the geothermal heat flow in the area varied between 50.02 and 85.1 mWm^{-2}, with the southern and northwest regions having the highest values.

Given the size of the Benue Trough, which encompasses the Lower, Middle, and Upper Benue Troughs and the associated costs, the majority of studies conducted were on a microscale in central Nigeria, primarily in the vicinity of the Middle Benue Trough. Other regions were not properly investigated at the time this study was conducted. Moreover, some of the techniques they used centered on data from ground magnetic surveying or data from wireline records from oil wells. These have the potential to limit certain sections that could have offered crucial details at specific places. This research paper's goal is to examine the prospects for geothermal energy in parts of the Benue trough (Middle and upper Benue trough) with wider coverage by employing spectral analysis techniques to analyze High-Resolution

Aeromagnetic data. This technique is employed because, in comparison with different approaches, it yields superior outcomes for depth estimation with fewer mistakes and allows estimations of depth, width, thickness, and magnetization [17]. The addition of this data on crustal temperature throughout the scope of the research area to the body of geothermal knowledge will support the push for the discovery and extraction of geothermal energy in the Northern location, which could provide an alternative source of energy production across the Nation, Northern Nigeria in particular.

2. THE LOCATION AND GEOLOGICAL BACKGROUND OF THE REGION OF RESEARCH

The region of coverage for the research is 166.5 km by 166.5km which is 27722.25 km^2 and lies within the Middle and Upper Benue Trough. It is situated between longitudes of 8°30'0''E and 10°00'0''E; latitudes of 8°00'0''N and 9°30'0''N. Geologically, the area of study coverage, Middle Benue Trough is underlain by sedimentary Basin and Basement Complex while Upper Benue Trough is mainly of Basement Complex. The Precambrian gneiss, migmatites, and metasediments that underlie the Basement Complex in Nigeria's Northern region have been invaded by a sequence of granitic rocks from the late Precambrian to the lower Palaeozoic [3].

Older Granite, a term for the plutonic rocks, was formed approximately 500–600 million years ago and represents the Pan-African orogeny in Nigeria. Mostly made up of granites, diorites, and dolerites, the older granites are Pan-African in origin. (800–400 Ma, i.e. Neo-Proterozoic to Early Palaeozoic). The most prevalent form of rock in the Nigerian Basement complex is the migmatite-gneiss complex (Figure 1a). Banded gneiss and biotite-gneiss comprised the majority of its composition. The biotitic gneisses, which are quite common, typically have significant foliation and fine grains due to the symmetrical arrangement of alternating dark and light minerals. The banded gneisses have complex band folding and alternate bands of light and dark color. The majority of the Basement complex is covered with belts of younger meta-sediments, which are significantly metamorphosed old pre-Cambrian sedimentary rocks that trend approximately north-south. The predominant geological formations in the region are the quartz-biotite-muscovite schist, which are relics of old shaly rocks. These metamorphose radially into micaceous schists with coarse grains that include feldspar. Commonly occurring schists include graphite, phyllites, and chlorite. Enormous spherical masses of older granite can be discovered within the older Migmatite gneiss complexes and schists are present across the Basement Complex. The ancient granites have a very different makeup. Younger granite complexes dominate the Jos Plateau in Nigeria, providing a unique assemblage of intrusive and volcanic rocks surrounded by ring faults or dykes.

Benue Trough is the Sedimentary Basin that underlies the study region. The Agwu-Ndeaboh Group, the Eze-Aku Group, the Nkporo Formation, and the Bima Formation are the Cretaceous sedimentary rocks that underlie the study region (Figure 1a). In the western edge of the Abakaliki Anticlinorium, the Eze-Aku Group is conformally overlaid by the Awgu Formation but the Nkporo Group underlies it in the Afikpo Synclinoium, with the Awgu Formation abruptly missing. Awgu Shale is made up of well-bedded, dark, bluish-grey shales with a profusion of thin limestone and marl interbeds. The Afikpo Sub-basin's base lithostratigraphic unit, the Nkporo Formation (Campanian–Maastrichtian), is primarily composed of dark grey to black shales, sandstone, some limestone, and oolitic ironstone beds [18].

In the Abakiliki Basin, a series of fossiliferous black shales and limestones make up the Awgu Formation. Shales, siltstone, sandstones, coals, and subsidiary limestone are interconnected in the Middle Benue Basin [19]. The oldest sedimentary unit in the Upper Benue Trough is the sandstone of the Bima formation. The bottom of the sedimentary sequence is made up of this Early Cretaceous Bima sandstone, which lies unevenly on the Pan African basement. The sandstone has uncommon sedimentary features and is not well-stratified [20]. Finer materials are filled on its internal scouring surfaces. The sandstone beds lack significant lateral consistency and have inconsistent connections. Predominantly composed of mudstones, shales, and coarse- to medium-grained sandstones embedded in carbonaceous clays, this formation was formed during continental circumstances (fluvial, deltaic, lacustrine).

3. MATERIALS AND METHOD

3.1. MATERIALS

Oasis Montaj 8.4, Arcmap 10.7.1, Matlab 7.5, and Surfer 14. The nine (9) Aeromagnetic datasets that were used include sheets.: Kurra (189), Pankshin (190), Wase (191), Wamba (210), Kwalla (211), Shendam (212), Afia (231), Akiri (232) Ibi (233) were acquired in digital format from the Nigerian Geological Survey Agency.

3.2. GEOPHYSICAL DATA PROCESSING METHOD

Fugro Airborne Surveys corrected all the aeromagnetic data. Geomagnetic gradient as well as diurnal variation were also taken care of from the aeromagnetic data [21] and were geo-referenced to the Universal Transverse Mercator (UTM) coordinate system. To reconcile the aeromagnetic data with the research area's geology map, they were georeferenced to the Universal Transverse Mercator coordinate system. Utilizing the Oasis Montaj 8.4 application, the first step involved combining the nine (9) aeromagnetic data sheets that covered the region of interest to create one database. From there, the single database was processed, filtered, and converted to different grid formats. It was then gridded using minimum curvature, and a Total Magnetic Intensity (TMI) map of the region was created (Figure 2) and exported to Arcmap10.7.1 to give the map a nice treat. First-order polynomial fitting was utilized to accomplish the residual extraction. The residual magnetic intensity anomaly (Figure 3a) was created using the magnetic anomalies' residual values. Before producing a power spectrum diagram for every block, the residual magnetic intensity anomaly map used in this research was divided into 25 spectral blocks with a 50% intersection of every block. Matlab 7.5 was then used to extract the depth to the top (Z_t) and depth to the centroid (Z_c) of the magnetic source from the spectral plots.

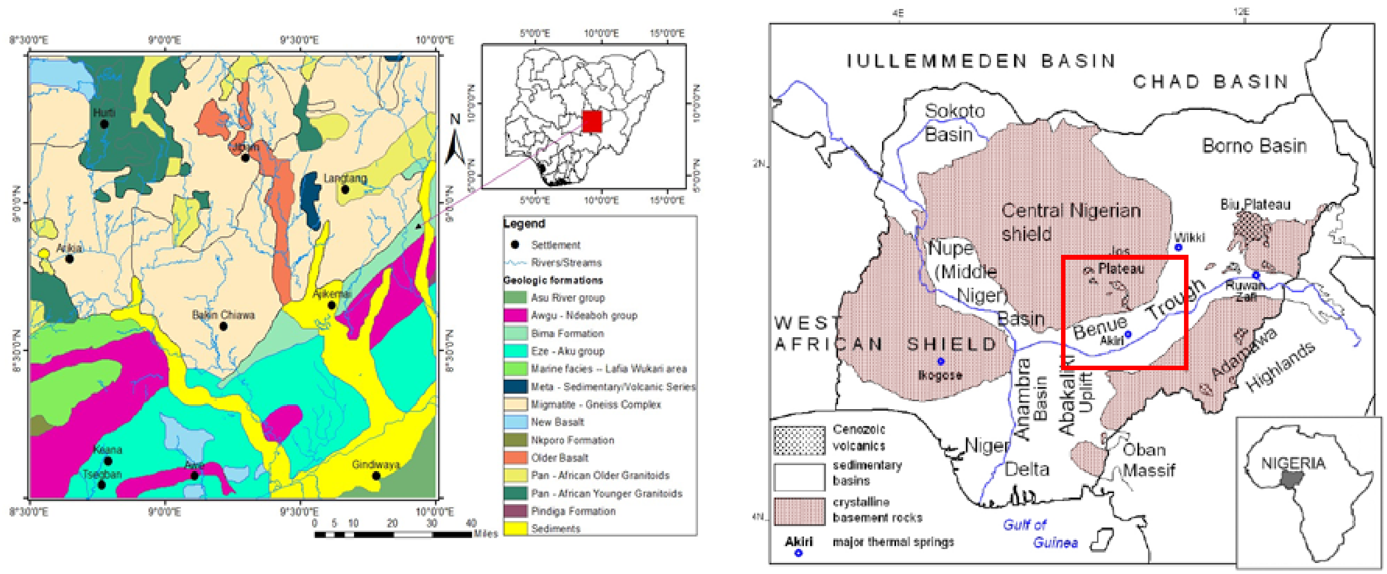

Figure 1. (a) Geological background within the region (b) Geological setting of Nigeria [3].

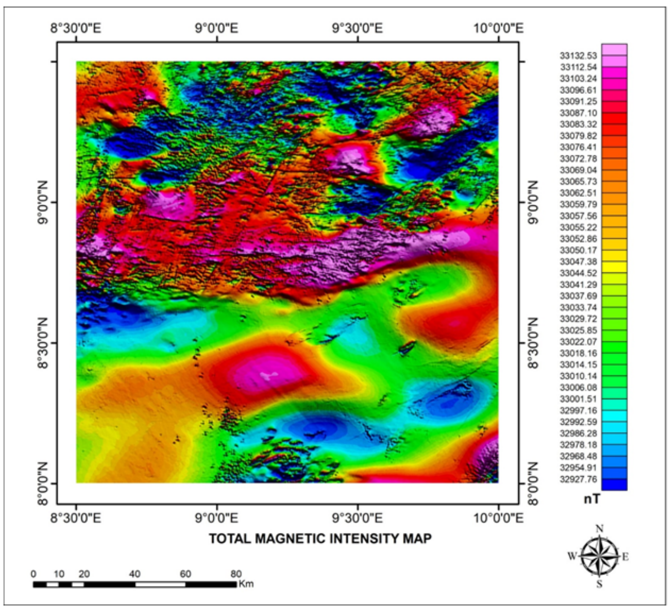

Figure 2. Total magnetic intensity map of the region.

3.3. *SPECTRAL ANALYSIS USING THE CENTROID DEPTH APPROACH FOR MAGNETIC ANOMALIES*

The process of figuring out and analyzing the spectrum of magnetic data is called spectral analysis. Throughout the years, it has been widely utilized to determine the depth of specific geological structures or the Curie isotherm [22, 23]. Magnetic anomalies' azimuthally averaged power spectrum is frequently used in its application [24].

The first step in doing the analysis is to use the gradient of the longest wavelength portion of the spectrum to estimate the depth to the magnetic source's center (Z_c). The depth to the magnetic center (Z_c) of the magnetic layer can be roughly estimated from the low-wavenumber region of the power spectrum [25];

$$In\left(p(k)^{1/2}/k\right) = InA - |k|\, Z_c. \tag{1}$$

As $(p\,(k))^{1/2}$ = power spectra of the magnetic anomalies, ln = natural logarithm,
$ln\left(p(k)^{1/2}/k\right)$ = radially averaged power spectrum of the magnetic anomalies, $|k|$ = wave number ($2\pi/\lambda$), and A = constant depending on the properties of magnetization and its orientation. The second step involves estimating the next longest wavelength spectral segment's depth to the top of the magnetic source (Z_t)[26]. Fitting a straight line through the intermediate to high wavenumber portion of the radially averaged power spectrum would allow one to determine the depth to the top of a magnetic source (Z_t) [27]. The magnetic layer's top depth (Z_t) corresponds to short wavelengths.

$$ln\left(p(k)^{1/2}\right) = InB - |k|\, Z_t. \tag{2}$$

$ln\left(p(k)^{1/2}\right)$ = radially averaged power spectrum of the anomaly, $|k|$ is the wave number(rad/km), and B = sum of constants independent of $|k|$. Equation 3 provides the Curie point depth of the magnetic source, which is obtained by combining the depths of the top and centroid. According to Ref. [25, 26] established a relation to determine the depth of Curie's point.

$$Z_b = 2Z_c - Z_t. \tag{3}$$

Assuming a constant temperature gradient ($\frac{dT}{dz}$) and a vertical direction for temperature change, Fourier's law applies in the unidimensional situation

$$q = -k\frac{dT}{dz}. \tag{4}$$

where q = heat flow (thermal transfer), k = coefficient of thermal conductivity. The depth to the Curie point (Z_b) with thermal gra-

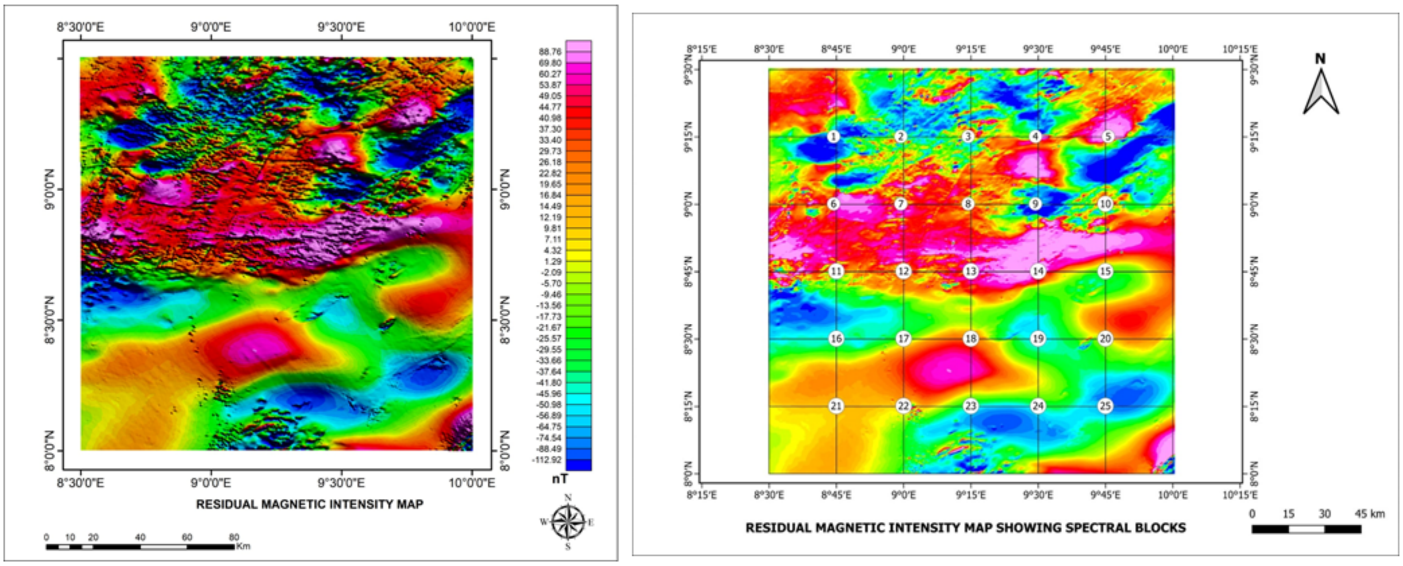

(a) (b)

Figure 3. (a) Residual magnetic intensity map of the region (b) Spectral blocks map.

dient ($\frac{dT}{dz}$) was used to compute the Curie temperature (θ) using the equation 4:

$$\theta = \left(\frac{dT}{dz}\right) Z_b, \tag{5}$$

$$And \left(\frac{dT}{dz}\right) = \frac{\theta}{Z_b}, \tag{6}$$

where$\left(\frac{dT}{dz}\right)$ is Geothermal gradient, Z_b in the absence of warmth sources, the surface temperature is 0°C, and dT/dz remains constant.

Heat flow is inversely proportional to any specified depth of a thermal isotherm [25]. Heat flow (HF) and geothermal gradient (GG) values, which were based on CPD estimations obtained from magnetic simulations, were computed using equations (4) and (6). Magnetic minerals determine the Curie point temperature. For instance, the Curie point temperature of magnetite (Fe2-xTixO3) is about 580 °C. The Curie temperature decreases as the titanium (Ti) percentage of titanomagnetite increases. The temperature of 580°C was used as the Curie point, and the thermal conductivity was 2.5 Wm^{-1} $°C^{-1}$.
Compared with eq. (6) after rearranging eq. (4)

$$z_b = \theta \frac{k}{q}. \tag{7}$$

According to eq. (7), Depth to the Curie point is inversely related to heat flow, meaning that locations with geothermal in-depth heat flow have more superficial Curie points, while areas with comparatively more superficial heat flows have in-depth Curie points [28].

4. RESULTS AND DISCUSSIONS

4.1. RESULTS

A TMI map is an embodiment of regional and residual magnetic fields. The deep-seated magnetic bodies give rise to the regional field, whereas the shallow-seated magnetic bodies (the field of interest) give rise to the residual field (Figure 2). The research area's primary source of the magnetic anomaly is contingent upon the magnetic characteristics and basement placements. Severe changes in the subterranean magnetic intensity were evident in the map, with the TMI values ranging from a lowest of 32927.76 nT to a peak of 33132.53 nT. The research area's areas with the highest TMI are indicated by the color pink in the color legend, while those with the lowest TMI within the study area are blue. High magnetic signature zone ranging from 33103.24 nT – to 33132.53 nT, the middle and northeastern parts of the map show a higher concentration of pink. Occurring alongside, are those ranging from 33047.38nT– 33096.61nT colored red and yellow. Low magnetic signature values ranging from 32927.76nT– 33001.51nT colored blue occur prominently in the Southern part and northern areas of the map alongside those ranging from 33006.08nT– 33044.52nT colored yellow and green. Variations in depth, lithological variations, dips and plunges, variations in magnetic susceptibility, and degree of the strike could all contribute to variations in magnetic field strength (those ranging from 33006.08nT– 33044.52nT colored yellow and green) [9]. Areas with minimal magnetic signatures (blue), intermediate magnetic features (yellow), and high magnetic signatures (pink) are represented on the residual magnetic intensity map of the study area (Figure 3a). High magnetic signature zones ranging from 33103.24 nT – 33132.53 nT colored pink are observed to occur more prominently in the central part and Northeastern areas of the map. The residual magnetic intensity values fluctuate between -112.92 nT and 88.76 nT, with some regions exhibiting strong favorable observable magnetic intensity values (pink color). The central portion of the map contains the majority of the short-wavelength magnetic anomalies. Short-wavelength magnetic signatures from the local rocks are generally low and high in the study area's magnetic anomalies. Table 1 displays the probable depth to the top (Z_t), depth to the centroid

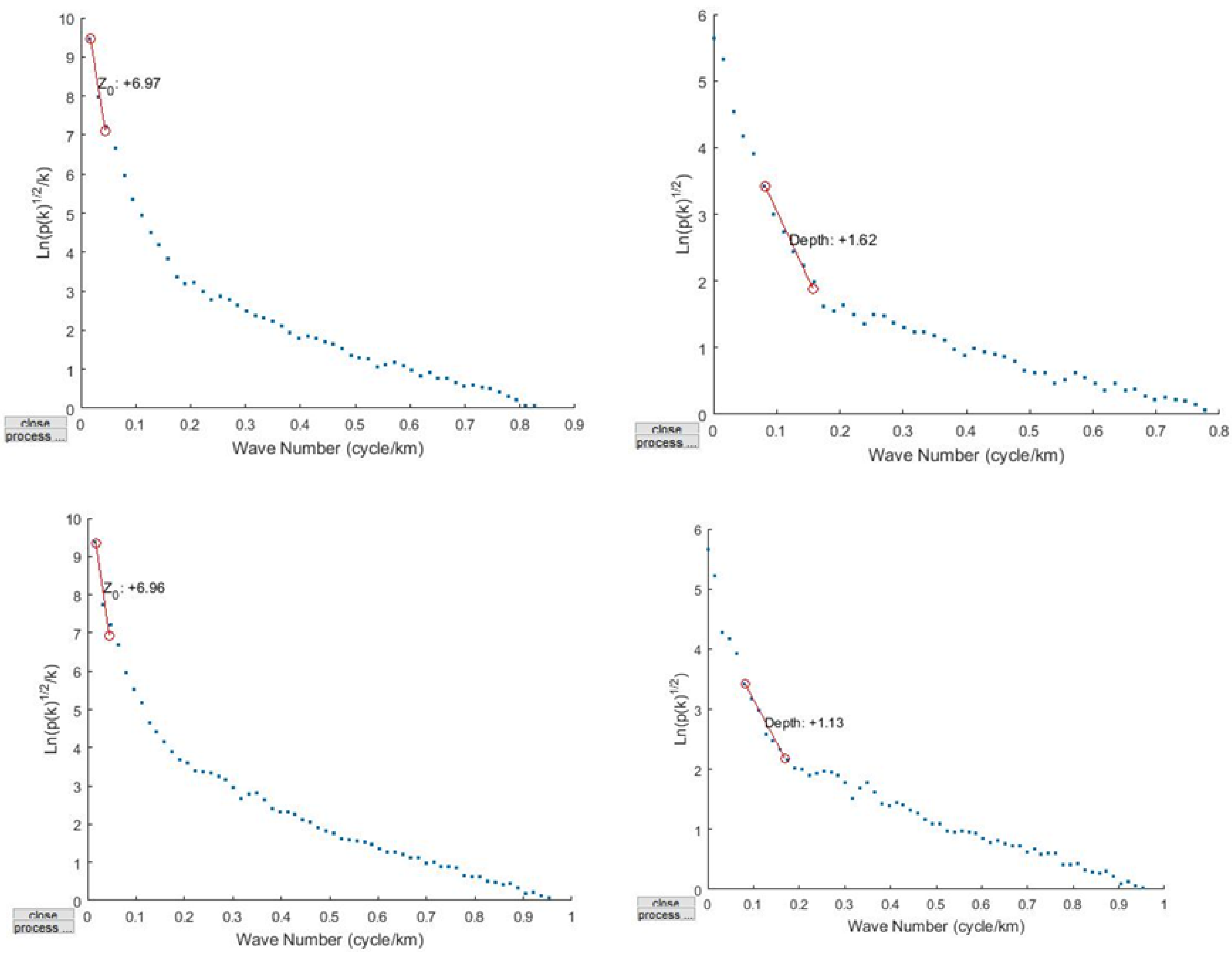

Figure 4. Graphs illustrating the logarithms of spectral energy versus wave numbers for B1 and B2 respectively.

(Z_0), Curie point depths (Z_b), geothermal gradient (dT/dZ), and geothermal heat flow(q). The spectral analysis result is presented in Figures 5, 6 and 7.

4.2. DISCUSSION

The variances in magnetic intensity that have been found, point to a variety of magnetic characteristics in the beneath rocks (Figure 2). Moreover, closures of magnetic highs may be the result of basic intrusion into the igneous/metamorphic basement rocks, thin sedimentary cover, shallow basement, another magnetic source, or thick sedimentary cover, which indicates a deep basement in that area [29]. The presence of extensive closures on the residual magnetic map (Figure 3a), which were composed of densely arranged linear sub-parallel alignments, suggested that local fractures or faults may have crossed these areas [21].

The results from spectral analysis (Table 1) show that the magnetic sources have a mean depth of 12.2068 km, ranging from 8.55 km to 16.38 km for the depth of the Curie point. This is the same as the research area's average magnetic source bottom depth (12.21 km). These results differ fairly as was recorded in some parts of the Middle Benue Trough of Nigeria [4] which ranges from 6.0 and 16 km, certain regions of Benue and Nasarawa state, which range from 9 km to 18.6 km, [10] and parts of the Middle Benue Trough(Shendam, Lafia, Akiri, Ibi, Makurdi, Akwana) ranges from 12.70 and 37.22 km, [30], Central Benue Trough Nigeria, ranges from 8.61 km to 36.04 km [15] did research within Middle Benue Trough region while some even beyond. The depths at which the thermal character of the crust is described are reflected in the Curie point depths. Places with volcanic and geothermal activity are characterized by Curie point depths less than or equal to 10 km [31]. Low curie point depths within the depth less than or equal to 10 km were found dominantly around the Northeast region of the study area (Figure 5). Magma upwelling and magmatic intrusion inside deeply fractured migmatite units and order granite units may be the reason behind the study area's shallow Curie point depth, while isostatic compensation or recovery could be the cause of the deeper Curie point in the southwest [21]. With a mean value of 48.85639 °C/km, the geothermal gradient varies from 35.40904 °C/km to 66.51376 °C/km. The heat flow value that is greatest is correlated

Table 1. The findings of spectral analysis. (Note: Italicize the greatest values, the lowest values are underlined).

Blocks	Long. (°)	Lat. (°)	Z_0(km)	Z_t (km)	Curie Depth (km)	GG (°Ckm^{-1}	Heat flow (mW)m^{-2}
B1	8.75	9.25	6.97	1.62	12.32	47.07792	117.6948
B2	9.00	9.25	6.69	**1.13**	12.25	47.34694	118.3673
B3	9.25	9.25	6.77	1.39	12.15	47.73663	119.3416
B4	9.50	9.25	5.83	1.16	10.5	55.2381	138.0952
B5	9.75	9.25	5.54	1.23	9.85	58.88325	147.2081
B6	8.75	9.00	7.09	1.23	12.95	44.78764	111.9691
B7	9.00	9.00	6.38	1.35	11.41	50.8326	127.0815
B 8	9.25	9.00	**5.08**	1.44	8.72	66.51376	166.2844
B9	9.50	9.00	5.48	1.92	9.04	64.15929	160.3982
B10	9.75	9.00	5.21	1.87	**8.55**	67.83626	169.5906
B11	8.75	8.75	7.43	1.59	13.27	43.70761	109.2690
B12	9.00	8.75	6.27	1.43	11.11	52.20522	130.5131
B13	9.25	8.75	7.89	1.71	14.07	41.22246	103.0561
B14	9.50	8.75	7.27	1.69	12.85	45.13619	112.8405
B15	9.75	8.75	6.29	1.31	11.27	51.46406	128.6602
B16	8.75	8.50	8.26	1.89	14.63	39.64457	99.11141
B17	9.00	8.50	7.4	1.39	13.41	43.2513	108.1283
B18	9.25	8.50	9.05	1.72	16.38	**35.40904**	**88.52259**
B19	9.50	8.50	6.63	1.98	11.28	51.41844	128.5461
B20	9.75	8.50	6.95	1.66	12.24	47.38562	118.4641
B21	8.75	8.25	8.81	1.32	16.3	35.58282	88.95706
B22	9.00	8.25	6.63	1.63	11.63	49.87102	124.6776
B23	9.25	8.25	6.64	1.23	12.05	48.13278	120.332
B24	9.50	8.25	7.92	1.4	14.44	40.1662	100.4155
B25	9.75	8.25	6.86	1.22	12.5	46.4000	116.0000
Average			6.8536	1.5004	12.2068	48.85639	122.1410

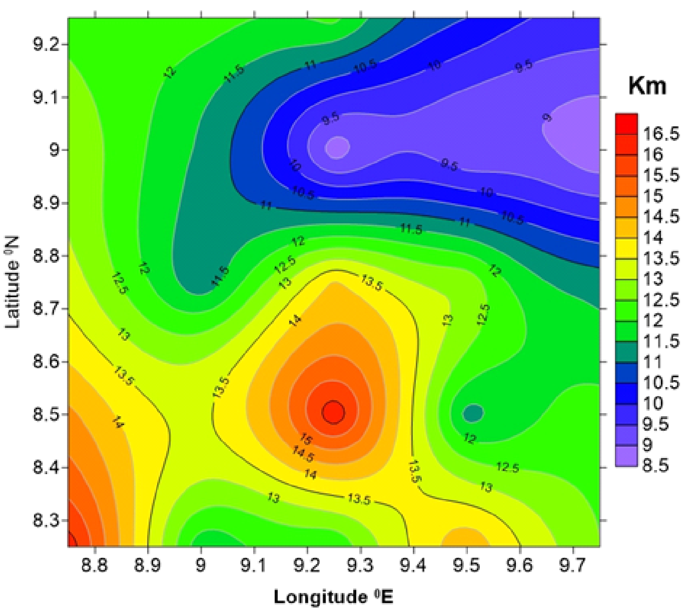

Figure 5. Curie point depth map (Contour interval∼.

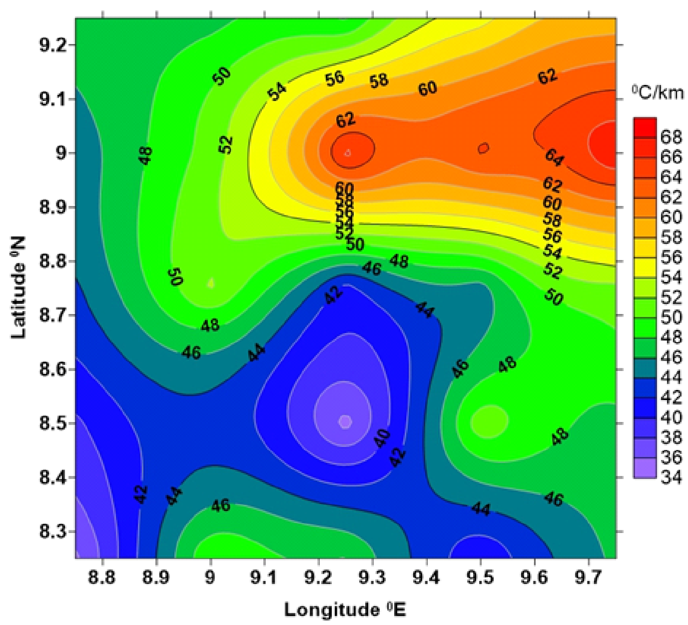

Figure 6. 2-D Geothermal gradient map (contour interval~2℃/*km*).

with the highest geothermal gradient value and the lowest value with the highest heat flow value. The geothermal heat flow values in the study area range from 88.52259 mW/m^2 to 166.2844 mW/m^2. The average heat flow in the area is 122.1410 mW/m^2. The heat flow map (Figure 7) shows that the study area is divided into areas with low and high heat flow. The values of the low heat

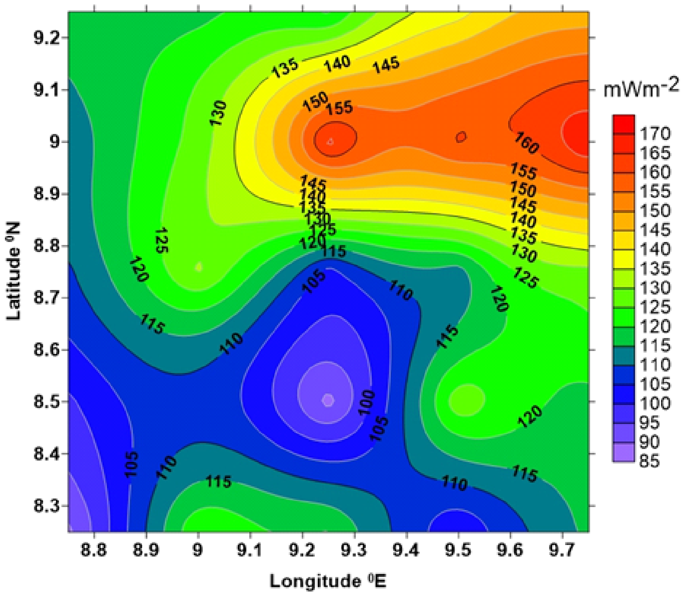

Figure 7. 2-D Heat flow map (contour interval~ 5mW/m^2).

flow areas range from 85 mW/m^2 to 95 mW/m^2 with progressive increase in geothermal gradient and heat flow towards the eastern direction which domesticated the highest heat flow from 135 mW/m^2 to 170 mW/m^2. The lowest heat flow value corresponds to the highest Curie point depth and vice versa. Heat flow is inversely proportional to a given isotherm thermal depth, as stated by [25]. This illustrates that, in contrast to the geothermal gradient, which varies linearly with heat flow, the Curie point varies inversely with heat flow. The main measurable factor in geothermal investigation has been heat flow.

Geologic evidence of strong heat flow, such as volcanic series supports the research area's heat flow conclusions. While the mean oceanic crust heat flow is 101 mW/m^2, the mean heat flow in a thermally normal continental crust is 60 mW/m^2 [32]. An excellent geothermal condition is indicated by heat flow rates ranging from 80 to 100 mW/m^2 [17]. A heat flow measurement above 100 mW/m^2 on the other hand indicates an unusual geothermal state [33]. The study area's heat flow measurements indicate that the crust is oceanic. Given the great thermal conductivity of the heat flow measured, the likelihood of a geothermal resource nearby is high. The result demonstrated that nearly the whole research region exhibits strong heat flow (>80 mW/m^2), suggesting the possibility of a geothermal energy source. Places with anomalous, low, and good geothermal gradient points correlate strongly with places with anomalous, low, and good heat flow regions, and vice versa, according to the geothermal gradient and heat flow contoured map.

5. CONCLUSION

With an average geothermal gradient of 48.85639 °C/km, the study area's average depth to the bottom of the magnetic source is 12.21 km. In the studied area, the values of geothermal heat flow vary from 88.52259 mW/m^2 to 166.2844 mW/m^2. The region's average heat flow is 122.1410 mW/m^2. The study area's heat flow measurements indicate that the crust is oceanic. Geologically, those areas with high heat flow are found within the basement complex. The research area's predominant geothermal and geotectonic features are consistent with the general trajectory of the heat flow. Analyses also reveal that Curie point depths are noticeably low in areas with a significant degree of geothermal signatures. As a result, it is widely accepted that places with strong geothermal signatures correspond to the lowest Curie point depth, whereas regions with the lowest heat flow value belong to the highest Curie point depth. Low Curie point depth regions could be associated with basic igneous or metamorphic rock intrusion, which would cause the nearby rocks to undergo hydrothermal alteration. Given the aforementioned features, these regions are presumably good sources of geothermal energy and are therefore advised for both geothermal exploration and utilization [25].

DATA AVAILABILITY

The data associated with this research can be obtained at https://drive.google.com/file/d/1PryobrYiEqkAU3roXNTdcFJJroDBZxaD/view?usp=sharing or at https://drive.google.com/file/d/1bXZ74Jktf4iM-qeLZeA1sdFRPxRg_bQa/view?usp=sharing.

References

[1] P. Newell & H. Bulkeley, "Landscape for change? International climate policy and energy transitions: evidence from sub-Saharan Africa", Climate Policy, Taylor & Francis Journals **17** (2016) 650. https://doi.org/10.1080/14693062.2016.1173003.

[2] C. Newsom, "Renewable Energy Potential in Nigeria: Low-Carbon Approaches to Tackling Nigeria's Energy Poverty", The International Institute for Environment and Development, London, UK, 2012, pp. 1–33. https://www.iied.org/sites/default/files/pdfs/migrate/G03512.pdf.

[3] E. Kurowska & K. Schoeneich, "Geothermal exploration in Nigeria", in proceedings of the World geothermal congress, Bali, Indonesia, 2010, pp. 25–29. https://www.geothermal-energy.org/pdf/IGAstandard/WGC/2010/1152.pdf.

[4] H. I. Alfaifi, S. E.Ekwok, A. Christian, C. A. Ulem, A. M. Eldosouky, S. Qaysi, K. Abdelrahman, P. Andráš & E.A. Akpan, "Exploratory assessment of geothermal resources in some parts of the Middle Benue Trough of Nigeria using airborne potential field data", Journal of King Saud University **35** (2022) 10252. https://doi.org/10.1016/j.jksus.2022.102521.

[5] I. I. Stylianou, G. Florides, S. Tassou, E. Tsiolakis & P. Christodoulides, "Methodology for estimating the ground heat absorption rate of Ground Heat Exchangers", Energy **127** (2017) 258. https://doi.org/10.1016/j.energy.2017.03.070.

[6] R. DiPippio, "Geothermal power plants: principles, applications, and case studies", Elsevier (2005) 263. https://doi.org/10.1016/B978-185617474-9/50043-1.

[7] E. B. Ikumbur, A. G. Onwuemesi, E. K. Anakwuba, A. I. Chinwuko & A. O. Usman, "Evaluation of geothermal energy potential of parts of the Middle Benue trough Nigeria: aeromagnetic and aeroradiometric approach", Iranian Journal of Geophysics **16** (2023) 37. https://doi.org/10.30499/ijg.2022.295242.1343.

[8] O. S. Ifeanyi, O. A. Ifeanyichukwu, C. P. Chidozie, A. C. Casimir, O. A Emeka & C. C. Agoha, "Solid mineral potential and geothermal energy reserve of northern basement complex, Nigeria", Materials and Geoenvironment **68** (2022) 1. https://doi.org/10.2478/rmzmag-2021-0017.

[9] A. Akiishi, B. C. Isikwue & A. T. Tyovenda, "Determination of geothermal energy sources in Masu Area Northeastern Nigeria using spectral analysis of aeromagnetic data", International Journal of Energy and Environmental Science **3** (2018) 89. https://doi.org/10.11648/j.ijees.20180305.11.

[10] T. D. Akinnubi & A. A. Adetona, "Investigation of the geothermal potential within Benue State, Central Nigeria, from radiometric and high-resolution aeromagnetic data", Nigerian Journal of Physics (NJP) **27** (2018). https://academia.edu/43786792/.

[11] I. G. Odidi, A. Mallam & N. Nasir, "Investigation of geothermal energy potential of parts of central and North-eastern Nigeria using spec-

tral analysis technique'', FUDMA Journal of Sciences (FJS) **4** (2020) 627. https://doi.org/10.33003/fjs-2020-0402-248.

[12] A. Mohammed, T. Adewumi, S. A. Kazeem, R. Abdulwaheed, A. A. Adetona & A. Usman, ''Assessment of geothermal potentials in some parts of upper Benue trough northeast nigeria using aeromagnetic data'', Journal of Geoscience, Engineering, Environment, and Technology **4** (2019) 7. https://doi.org/10.25299/jgeet.2019.4.1.2090.

[13] S. O. Ibe & K. I. Uche, ''Assessment of geothermal energy potential of Ruwan Zafi, Adamawa State and Environs, Northeastern Nigeria, using High-Resolution Airborne Magnetic Data'', Current Research in Geoscience **10** (2020) 1. https://doi.org/10.3844/ajgsp.2020.1.15.

[14] F. C. Anyadiegwu & C. O. Aigbogun, ''Curie point depth, heat flow and geothermal gradient determined from analysis of aeromagnetic data over parts of the lower benue trough and anambra basin, Nigeria'', J. Appl. Sci. Environ. Manage **25** (2022) 1821. https://doi.org/10.4314/jasem.v25i10.10.

[15] . G. N. Egwuonwu, E. K. Nnaemeka & O. Orji, ''Investigating the geothermal energy potentials within the central Benue trough Nigeria: insight from airborne potential field data'', International Journal of Innovative Science and Research Technology **8** (2023) 2456. https://doi.org/10.5281/zenodo.7858900.

[16] K. A. I. Salako, A. A. Adetona, A. A. Rafiu, U. D. Alahassan, A. Aliyu & T. Adewumi, ''Assessment of geothermal potential of parts of middle benue trough, North-East Nigeria'', Journal of the Earth and Space Physics **45** (2020) 27. https://doi.org/10.22059/jesphys.2019.260257.1007017.

[17] M. B. Yakubu, K. M. Lawal, B. B. M Dewu & A. E. Ikpokonte, ''Investigation of geothermal energy resource potential using aero-magnetic and aeroradiometric data of Kano, Nigeria'', FUDMA Journal of Sciences (FJS) **6** (2022) 296. https://doi.org/10.33003/fjs-2022-0601-900.

[18] A. Simpson, ''The Nigerian coal field: The geology of parts of Onitsha, Owerri, and Benue Provinces'', Geological Survey Nigeria Bulletin **24** (1954) 1. https://www.scirp.org/reference/referencespapers?referenceid=1748382.

[19] J. Benkhelil, ''The origin and evolution of the Cretaceous Benue Trough, Nigeria'', Journal of African Earth Sciences (and the Middle East) **8** (1989) 251. https://doi.org/10.1016/S0899-5362(89)80028-4.

[20] J. D. Carter, W. Barber, E. A. Tait & G. P. Jones, ''The geology of parts of adamawa, bauchi and borno provinces in northeastern nigeria'', Geological Survey of Nigeria Bulletin **30** (1963) 1. https://www.scirp.org/reference/referencespapers?referenceid=1266818.

[21] E. Ike, A. S. Oniku, S. C. Ezike & R. E. Wilson, ''Lithological and structural mapping of parts of southwestern Nigeria using aeromagnetic data'', Recent Advances in Natural Sciences **2** (2024) https://doi.org/10.61298/rans.2024.2.1.54.

[22] A. Spector & F.S. Grant, ''Statistical models for interpretation of aeromagnetic data'', Geophysics **35**(1970)293. https://doi.org/10.1190/1.1440092

[23] A. Tanaka, ''Global centroid distribution of magnetized layer from world digital magnetic anomaly map'', Tectonics **36** (2017) 3248. https://doi.org/10.1002/2017TC004770.

[24] R. T. Shuey, D. K. Schellinger, A. C. Tripp & L. B. Alley, ''Curie depth determination from aeromagnetic data spectral analysis'', Geophysical Journal **50** (1977) 75. https://doi.org/10.1111/j.1365-246X.1977.tb01325.x.

[25] A. Tanaka, Y. Okubo & O. Matsubayashi, ''Curie point depth based on spectrum analysis of the magnetic anomaly data in East and Southeast Asia'', Tectonophysics **306** (1999) 461. https://doi.org/10.1016/S0040-1951(99)00072-4.

[26] Y. Okubo, J. R. Graf, R. O. Hansen, K. Ogawa & H. Tsu, ''Curie point depths of the island of kyushu and surrounding areas'', Geophysics **53** (1985) 481. https://doi.org/10.1190/1.1441926.

[27] I. Amin, A. S. Saada, M. Kevin, A. Kamal & I.K. Fares, ''Comparative study of estimating the Curie point depth and heat flow using potential magnetic data'', De Gruyter **14** (2022) 462. https://doi.org/10.1515/geo-2022-0378.

[28] H. E. Ross, R. J. Blakely & M.D. Zoback, ''Testing the use of aeromagnetic data for the determination of curie depth in California'', Geophysics **71** (2006) L51. https://doi.org/10.1190/1.2335572.

[29] B. E. Eletta & E. E. Udensi, ''Investigation of the curie point isotherm from the magnetic fields of the eastern sector of central Nigeria'', Journal of Geosciences **4** (2012) 101. http://dx.doi.org/10.5923/j.geo.20120204.05.

[30] E. B. Ikumbur, A. G. Onwuemesi, E. K. Anakwuba, A. I. Chinwuko & A. O. Usman, ''Evaluation of geothermal energy potential of parts of the middle Benue trough Nigeria: aeromagnetic and aeroradiometric approach'', Iranian Journal of Geophysics **16** (2023) 37. http://dx.doi.org/10.30499/ijg.2022.295242.1343.

[31] J. A. Bulus & O. K. Likkason, ''Estimation of curie point depths and succeeding geothermal parameters from high-resolution aeromagnetic data of the younger granite complexes of Jos and environs Northcentral Nigeria'', Science World Journal **16** (2021) 232. https://www.ajol.info/index.php/swj/article/view/221734.

[32] C. Jaupart & J. C. Mareschal, ''Heat flow and thermal structure of the lithosphere'', Institut de Physique du Globe de Paris, Paris, France, GEOTOP-UQAM-McGill, Montreal, QC, Canada, 2007, pp. 218–250. https://booksite.elsevier.com/brochures/geophysics/PDFs/00104.pdf.

[33] A. Jessop, M. Hobart & J. Sclater, ''The World heat flow data collection 1975'', Geothermal Services of Canada **50** (1976) 55. https://doi.org/10.4095/8416.